A Measurement Fixture Suitable for measuring Substrate Noise in the UWB Frequency Band

Shen, Ming; Tong, Tian; Mikkelsen, Jan H.; Larsen, Torben

Published in:
Analog Integrated Circuits and Signal Processing

DOI (link to publication from Publisher):
10.1007/s10470-008-9181-x

Publication date:
2009

Document Version
Accepted author manuscript, peer reviewed version

Analog Integr Circ Sig Process (2009) 58:11–17
DOI 10.1007/s10470-008-9181-x

A measurement fixture suitable for measuring substrate noise in the UWB frequency band

Ming Shen · Tian Tong · Jan H. Mikkelsen · Torben Larsen

Received: 11 February 2008 / Revised: 8 April 2008 / Accepted: 17 April 2008 / Published online: 4 June 2008

Abstract This paper presents a measurement fixture suitable for measuring substrate carried noise for lightly doped substrates within the UWB frequency band. Signals coupling through the substrate are usually fairly weak and special precautions are taken to avoid any distortions that may be caused by the test fixture. The proposed measurement fixture is based on a modified ground-signal-ground (GSG) pad fixture. Parasitic effects in the measurement fixture are evaluated with help of an equivalent circuit model. From measured results, the presented fixture is shown to provide a measurement band from 3 to 10 GHz. As an example of the usability of the presented fixture a test-case using a class-E PA is presented. The noise injected by the class-E PA is measured using the proposed fixture as noise detector and the results are show to be accurate to within ±1.5 dB.

Keywords Wide band measurements · Substrate noise · UWB · GSG

M. Shen (✉) · T. Tong · J. H. Mikkelsen · T. Larsen
Technology Platforms Section, Department of Electronic Systems, Aalborg University, Aalborg, Denmark
e-mail: mish@es.aau.dk

T. Tong
e-mail: tt@es.aau.dk

J. H. Mikkelsen
e-mail: jhm@es.aau.dk

T. Larsen
e-mail: tl@es.aau.dk

1 Introduction

UWB communication is one of the technology platforms currently being investigated in support of both low data rate and high data rate applications. It is considered to be one of the most promising wireless technologies for short-range systems [1]. Due to an advantage in cost and device density, CMOS technologies, especially lightly doped technologies, hold a great potential of complying with the needs for cheap and compact implementation of UWB devices. However, UWB systems demand stringent noise figure owing to its ultra wideband nature (larger than 500 MHz within the allocated frequency band from 3.1 to 10.6 GHz) and the low power spectral density of the signal [2]. The noise issue is of particular concern for UWB systems implemented on a single chip as substrate noise here will further degrade performance. In such scenarios, sensitive RF circuits such as low noise amplifiers have to be integrated together with noisy circuits, such as digital circuits, switch-mode power amplifiers, frequency dividers etc. Those noisy circuits result in the generation of substrate noise in a wide frequency band. Due to the low resistivity of the substrate (10–20 Ohm-cm for lightly doped substrates), the substrate noise can easily propagate to the RF circuit area and deteriorate the noise figure.

While it may be easy to conceptualize the coupling through the substrate, it is much more difficult to measure this noise in any real circuit. This is especially the case measurements are needed for in an ultra wide frequency band where the valid measurement frequency band usually is limited by the parasitic effects in the measurement setup. So far, a number of studies have been conducted on the measurement of substrate noise [3–11]. The reported studies attempt to address the problem of substrate noise measurement from different perspectives. Some try to

verify the coupling model of the substrate [3–5]; some focus on heavily doped CMOS or other integrated circuit processes [6–8]; some investigate the waveforms or narrow band power spectral density (PSD) of substrate noise [9]; while others propose complicated circuits or devices as substrate noise sensors [10, 11]. However, few publications have investigated an appropriate wide band measurement method for measuring substrate noise in UWB systems implemented using lightly doped CMOS processes.

This paper presents a measurement fixture that is suitable for measuring substrate carried noise for lightly doped substrates within the UWB frequency band. The aim is here to obtain a measurement of the wide band PSD of the substrate noise. A measurement fixture based on a modified GSG pad is shown to have high potential for accomplishing this. A test chip is designed using a 0.18 μm lightly doped CMOS process to evaluate the effects of two key parasitic factors, the distance-based substrate resistance and the capacitance between the substrate and the Metal_1 ground. Several practical design rules for reducing the parasitical effects are concluded based on measurement results. As an example of the usability of the proposed method, switching noise measurements are presented for a switch-mode class-E PA.

This paper is organized as following: Sect. 2 describes the substrate noise measurement fixture. Section 3 discusses the evaluation of the effects of different measurement distances and the capacitive coupling between the substrate and the Metal_1 ground plane of the measurement setups. Section 4 presents the experiment on measuring of switching noise generated by a class-E PA. In Sect. 5 conclusions are drawn.

2 The substrate noise measurement fixture

To experimentally investigate the substrate noise in an UWB system, the measurement setup must have a sufficiently wide measurement bandwidth. It is therefore important to avoid introducing complicated parasitic components or devices in the measurement setup, which can dramatically affect the measurement results. The presented substrate noise measurement fixture, also refered to as the substrate noise detector, is designed based on a modified GSG pad structure composed of two 85 × 85 μm ground pads and one 85 × 85 μm signal pad. The center-to-center distance between the signal pad and each ground pad is 150 μm. Thus, no extra fixture apart from a GSG probe is needed for the measurement of the substrate noise. The cross section view of the fixture is shown in Fig. 1. For simplicity only one metal layer, the Metal_1 layer, is shown here. In the actual setup all metal layers are connected to the top metal layer.

It should be noted that the signal pad is directly connected to the substrate while the ground pads are not connected to the substrate. There are two reasons for this:

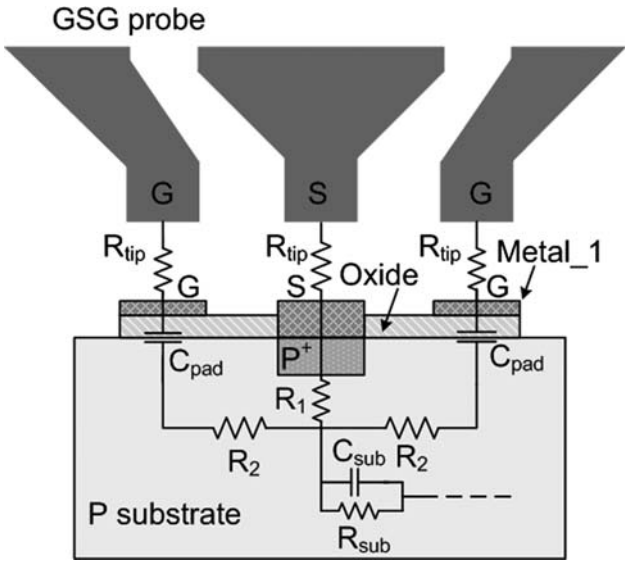

Fig. 1 Cross-section view and the equivalent circuit of the substrate noise measurement fixture

(1) Substrate noise is generally low power and therefore it is better to connect the signal pad as directly as possible to the substrate to minimize loss. Besides, this can establish a wide band resistive detection path of substrate noise since the substrate is modelled as a purely resistive network.
(2) If the ground pads also are connected to the substrate, then the measured signal becomes a differential mode signal of the substrate noise detected by the signal pad and the ground pads. It is expected to be very small since the signal pad and ground pads are located close to each other.

Figure 1 also shows the equivalent circuit model of the substrate noise measurement fixture. R_{tip} is used to model the contact resistance associated with the probing. The Metal_1 ground pad and the substrate is isolated by the oxide layer which comprises the oxide capacitance that is modelled by C_{pad}. The capacitance between the signal pad and the ground pad is significantly smaller than C_{pad} and thus neglected. It should be noticed that C_{pad} is the only reactive component in the model and the bandwidth of the measurement fixture is closely related to its value. Its value can be approximately calculated from the oxide thickness and the pad dimensions by

$$C_{pad} = W \cdot L \cdot \frac{\varepsilon_{ox}}{t_{ox}}, \tag{1}$$

where W, L are the width and the length of the pad respectively, and ε_{ox} and t_{ox} are the permittivity and thickness of the oxide layer between the pads and the substrate, respectively.

For lightly doped processes, the substrate can not be treated as one single node like the case is for heavily doped substrates [8]. To account for this, R_1, R_2, C_{sub} and R_{sub} are added to form a simplified network model of the substrate.

R_1 and R_2 are used to model the spreading resistance of the substrate below the signal pad and the ground pad. R_{sub} and C_{sub} are used to model the resistive and capacitive coupling between the substrate noise source and the measurement fixture. The values of R_1, R_2 and R_{sub} are difficult to precisely estimate from available parameters and are therefore derived from experimental data.

3 Evaluation of parasitic effects

In practical measurements of substrate noise, the substrate noise propagating from the noise source to the measurement point experiences attenuation and distortion. Distance-based substrate resistance and capacitive coupling between the substrate and the ground of the measurement setup are two key factors responsible for these effects. In order to obtain accurate measurements of the substrate noise, it is necessary to study the effects of such parasitics.

3.1 Design of the test chip

Based on the substrate noise measurement fixture in Sect. 2 a test chip has been designed to evaluate the effects of distance-based substrate resistance and the capacitive coupling between the substrate and Metal_1 ground. Figure 2 shows the topology of the test chip. Four substrate noise detectors (denoted A, B, C and D) are placed with separating distances of 230, 300 and 300 μm, respectively. For each signal pad and ground pad, all the available metal layers from Metal_1 to Metal_6 are connected. Two wide metal strip lines composed of Metal_1 connect ground pads of the substrate noise detectors to produce capacitive coupling between the substrate and the ground of the measurement setup.

Figure 3 shows an equivalent circuit model of the test structure. Here, there are four sub-circuit networks indicated by four dashed squares. Network 1 and 2 are models of the substrate noise detectors at port 1 and port 2. Network 3 is the model of the forward coupling network between the two measurement ports, including resistive coupling and capacitive coupling. Network 4, composed of C_{strip}, R_3 and L_{strip}, is used to model the coupling between

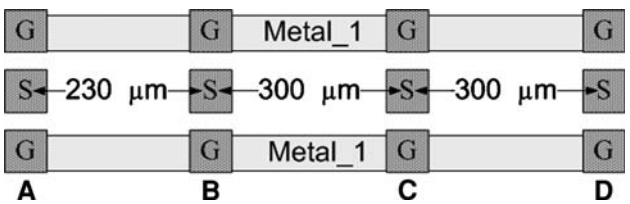

Fig. 2 Topology of the test structure for evaluation of parasitical effects

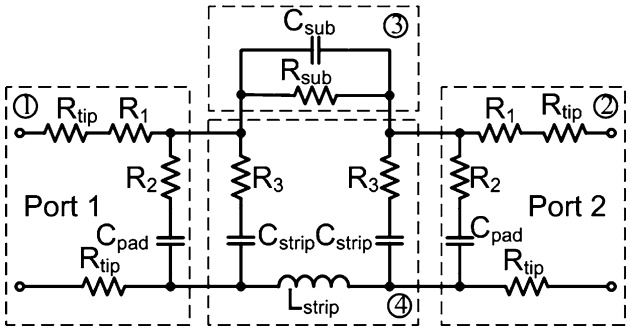

Fig. 3 The equivalent circuit model of the test structure in Fig. 2

the Metal_1 ground strip lines and the substrate. Similar to C_{pad} in the model of the noise detector, C_{strip} can be roughly calculated from the oxide thickness and the strip dimensions. However, for the test structure in Fig. 2 the dimension of the ground strip is so large that the electric field between it and the substrate can not be treated as a uniform field and therefore needs more consideration. Figure 4 shows the results of an EM simulation of the electric field in the oxide layer beneath the ground strips using the finite element method. A 6 GHz signal source is placed on the signal pad of noise detector A in Fig. 2 to excite the simulation. The electric field is shown using a 1-D electric field curve taken from the oxide layer beneath one of the ground strips in Fig. 2. It can be seen that the strength of the electric field decreases quickly as the distance between the observing point and the noise detector increases. This means that C_{strip} is over-estimated if its value is calculated using the actual length of 915 μm.

From Fig. 4, it can be seen that the electric field remains at a high level for distances of 50 μm and then drops quickly as the distance increases. Therefore, for calculating C_{pad}, the length, L, is decided as 50 μm and the width, W, is 85 μm. Then the oxide capacitance for one ground pad is calculated as 127.5 fF. Consider that two ground pads are placed in parallel, the value of C_{pad} is decided as shown in Table 1. Moreover, the electric field is found concentrated within a

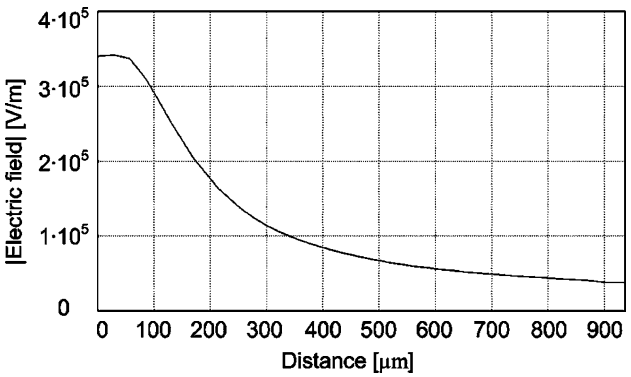

Fig. 4 1D simulated electric field in the oxide layer beneath the ground strip line in Fig. 2

Table 1 Parameters of the equivalent circuit in Fig. 3 (R_1, R_2, R_3 and R_{sub} are derived from experimental data; C_{pad} and C_{strip} are calculated based on Eq. 1 and simulated results in Fig. 4; C_{sub}, R_{tip} and L_{strip} are fitted variables)

Items	AB	BC	BD
R_{sub} (Ω)	80	100	130
C_{sub} (fF)	30	20	10
R_{tip} (Ω)	3	3	3
R_1 (Ω)	140	140	140
R_2 (Ω)	40	40	40
R_3 (Ω)	60	30	10
C_{pad} (fF)	250	250	250
C_{strip} (fF)	1800	2000	2400
L_{strip} (pH)	1	1	1

distance of 480 μm, which indicates the main area where the capacitive coupling happens. Thus it is reasonable to calculate C_{strip} according to this distance. For example, the length, L, is decided as 380 μm, subtracting $2 \times 50 = 100$ μm from 480 μm, for the case of AB. Then the C_{strip} for the case AB is calculated as 1.94 pF and finally decided as 1.8 pF due to the decreasing of the electric field. Similarly, C_{strip} for the case of BC and BD are decided as shown in Table 1. L_{strip} is the inductance of the strip line. Generally, the value of L_{strip} is small and 1 pH is used in the equivalent circuit.

3.2 Measurement of the DC resistances

To determine the distance dependency of the substrate resistance, the DC resistance between the different signal pads of noise detector A, B, C and D are measured and the results are shown in Fig. 5. The DC resistances with distance of 230 μm (AB), 300 μm (BC), 530 μm (AC) and 600 μm (BD) are measured as 360 Ω, 380 Ω, 405 Ω and 410 Ω, respectively. It is seen that the resistances are on the order of hundreds of Ohms and the variation of the resistances is insignificant. This indicates that, for measurement distances from 230 μm to 600 μm, the attenuations caused by substrate resistances are large but fairly constant. Furthermore, the values of R_1 and R_{sub} in the equivalent circuit of Fig. 3 are derived based on these measurement results. For instance, in the case of BC, the value of $2 \cdot R_1 + R_{sub}$ is decided as 380 Ω, which equals the measured DC resistance. Since the ground pads are not connected to the substrate, it is difficult to measure the spreading resistance between the signal pad and the ground pad. But its value can be approximated based on the measured DC resistances in Fig. 5. The ground pads have the same dimensions as the signal pads and the central to central distance is 150 μm. So the spreading resistance of the substrate below the signal pad and the ground pad can be approximately decided as 360 Ω. Further, considering that two ground pads are connected in parallel. the spreading resistance values of R_2 and R_3 are approximated as shown in Table 1.

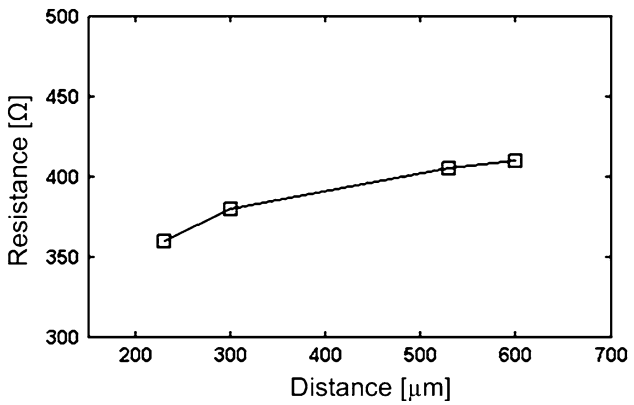

Fig. 5 Measured DC resistances on the test chip of Fig. 2

3.3 Measurement of S-parameters

To determine the frequency dependency of the propagation effects, the test chip is studied using S-parameter measurements over 45 MHz to 10 GHz. The measured S21s over distances of 230 μm (AB), 300 μm (BC) and 600 μm (BD) are illustrated in Fig. 6. The simulation results of the equivalent circuit with parameters in Table 1 are also shown in Fig. 6. From these results the equivalent circuit model is seen to match measured data accurately, especially in case AB and BC. Relatively larger deviations are seen in case BD. For this case, the magnitude of S21 is around −45 to −50 dB at high frequencies, which makes accurate measurement a non-trivial task. And thus a reduced accuracy is expected over high frequencies. It is also seen in Fig. 6(a) that the attenuations at 45 MHz with different distances are almost identical at −14 dB. For such a low frequency, all capacitive couplings can be approximately treated as open circuit and the attenuation is mainly caused by the substrate resistance. Since the values of the substrate resistances of different distances are similar the attenuations are of course similar too.

Moreover, high attenuations are observed at high frequencies. For instance, attenuations of −32, −38 and −47 dB are observed at 8 GHz for the three different cases. From Table 1, it is noticed that R_{sub}, C_{sub}, R_3 and C_{strip} are the only four changing variables that might be responsible for this. C_{sub} is insignificant due to its small value. R_{sub} is also excluded by reason of its near constant value in the three cases. Thus the different attenuations over high frequencies of three cases must be resulted from different values of R_3 and the intentionally built capacitances between the Metal_1 ground strip lines and the substrate, i.e. C_{strip}. For higher frequencies, coupling through R_3 and C_{strip} to ground is more

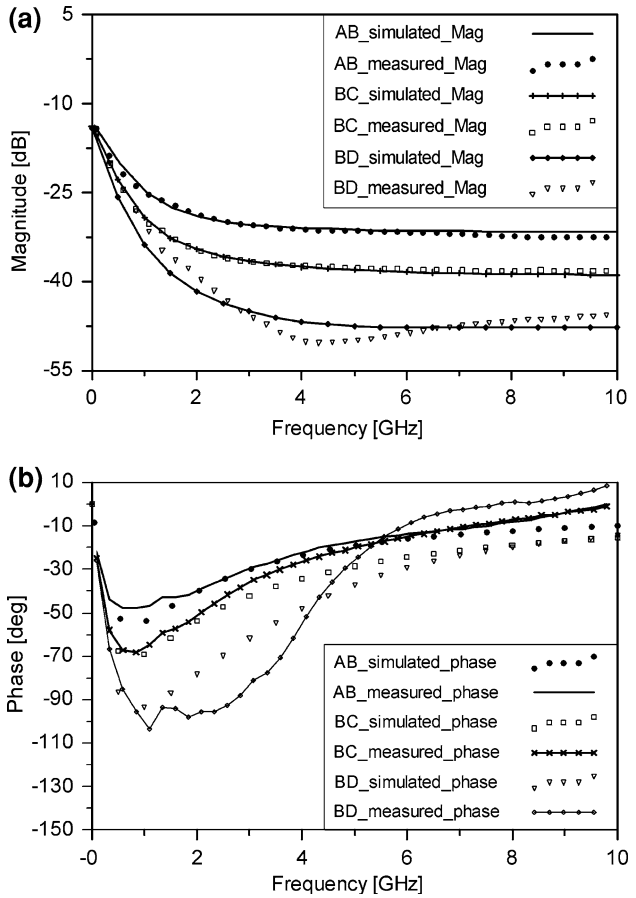

Fig. 6 Simulated and measured (**a**) Magnitudes and (**b**) Phases of S21 of the test structures in Fig. 2

pronounced than that of low frequencies and thus the magnitude of S21 decrease. However, all S21 magnitude responses are flat over the frequency band of 3 to 10 GHz (with fluctuation less than 3 dB), which means the measurement setup can be used to measure the PSD of substrate noise even under conditions of strong parasitic effects.

Considering the measured S21 in Fig. 6 and the corresponding values of R_3 and C_{strip} in Table 1, it is seen that a larger R_3 and a smaller C_{strip} helps to decrease the loss. Then several design rules of the presented measurement fixture in practical applications can be drawn as following. The value of R_3 should be increased by reducing the dimensions of the ground pads on Metal_1 layer but keep the size of 85 × 85 μm on the top metal layer for measurement purpose; C_{strip} should be reduced by deleting the Metal_1 ground around the noise detector or using the top metal layer to connect the ground pads. Moreover, Since the distance-based substrate resistances for measurement distances from 230 to 600 μm are similar, distance is not a key factor to avoid significant attenuation. A long distance between the substrate noise source and the noise detector like 600 μm is acceptable if needed for other purposes such as convenient probing.

4 Experiment on measuring substrate noise generated by a class-E PA

As a practical example, the presented substrate noise measurement fixture is used to measure the switching noise generated by a switch-mode class-E PA. The class-E PA is designed in the same 0.18 μm technology as the test chip in Sect. 3 and hence all conclusions and design rules drawn above can be applied. In this experiment, the PA acts as a switching noise source and the proposed measurement fixture as noise detector. When the PA is driven by high frequency signals, the generated switching noise occupies a wide frequency band, which makes it a suitable signal source to validate the wide band characteristic of the measurement fixture. Moreover, when the PA is switching on and off, the switching current is injected into the substrate mainly through the junction capacitor at the drain of the biggest NMOS transistor in the PAs output stage as shown in Fig. 7. Since the junction capacitance of the NMOS transistor is big, it is here treated as short circuit for high frequencies and the signal at the drain node is coupled into the substrate without significant distortion. Thus the switching noise measured at the substrate noise detector can be compared with the signal measured at the drain node to find out the distortion caused by the substrate noise detector over a very wide frequency band.

While designing the substrate noise detector on the chip, several factors are taken into account. Firstly, to have a clean reference ground, the substrate noise detector's ground is closely connected to the ground pad of the DC supply. Secondly, for convenient probing, the substrate noise detector is placed at the edge of the chip with a distance of approximately 600 μm to the output stage of the class-E PA. Finally, following the design rules drawn in Sect. 3, to avoid large attenuations, the Metal_1 ground plane around the substrate noise detector is deleted to reduce the capacitance between the Metal_1 ground plane and the substrate. The chip photo is shown in Fig. 8.

Firstly, the frequency spectrum of the signal at the drain node of the PAs output stage is measured when the class-E

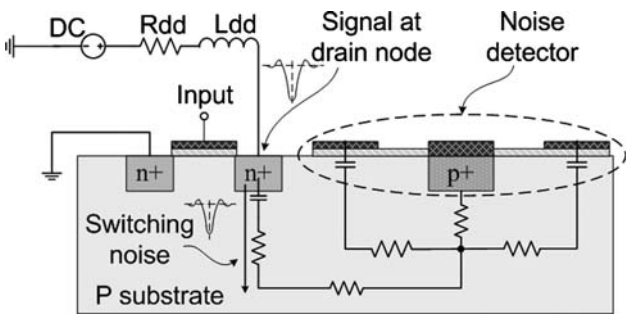

Fig. 7 Simplified topology of the experimental chip

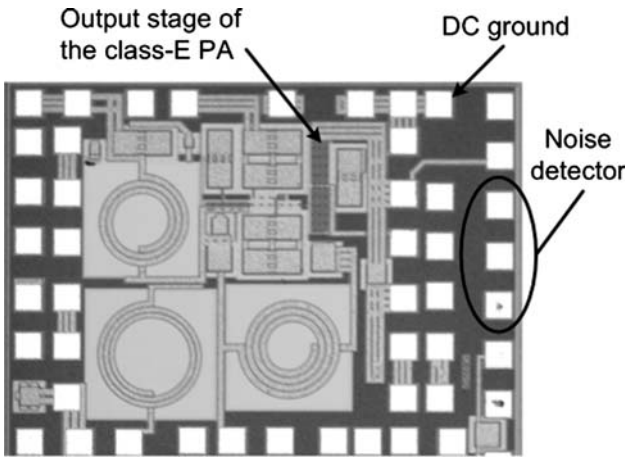

Fig. 8 Chip photo of the class-E PA and the substrate noise detector

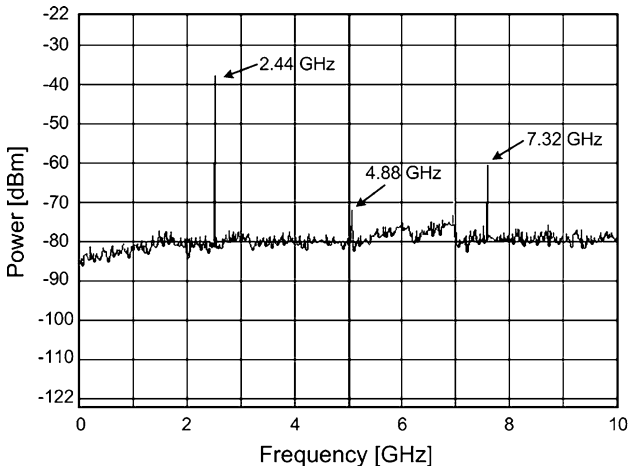

Fig. 9 Frequency spectrum of the switching noise of the class-E PA measured using noise detector

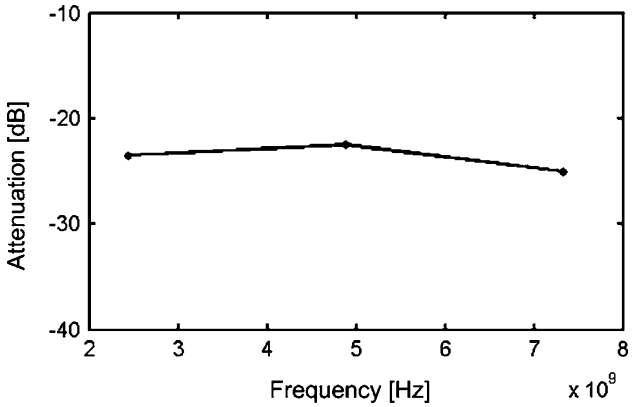

Fig. 10 Attenuations caused by the noise detector in the band 2.44–7.32 GHz

PA is operating at maximal output power. Three discrete spectral components are measured at 2.44, 4.88 and 7.32 GHz, i.e. the fundamental and harmonics of the signal, with magnitudes of −12.5, −49.5 and −35 dBm, respectively. The fourth harmonic at 9.76 GHz is too weak to be measured. But the three spectral contents already cover a wide frequency band, which makes it usable for verifying the wide measurement bandwidth of the measurement fixture.

Based on the assumption that the signal at the drain node is coupled into the substrate without significant distortion, the substrate noise measured at the noise detector is expected to have a similar frequency profile except suffering from certain resistive attenuations. To verify this, the substrate noise is measured at the noise detector and the result is presented in Fig. 9. It shows that the spectral contents of the measured substrate noise appear at 2.44, 4.88 and 7.32 GHz with magnitudes of −36, −72 and −60 dBm, respectively. Then the attenuations for each component from the drain node to the noise detector are found to be −23.5, −22.5 and −25 dB, respectively. As shown in Fig. 10, it can be seen that the attenuation profile is quite flat in the band of 2.44–7.32 GHz with an average value of −23.75 dB and variation of ±1.25 dB. This validates the wide band characteristic of the presented measurement method.

5 Conclusion

A measurement fixture is presented for the measurement of substrate noise in lightly doped substrates within the UWB frequency band. The effects of the distance-based substrate resistance and the capacitive coupling between the substrate and the ground are evaluated by measurement of a test chip. An equivalent circuit model of the measurement fixture is given and shows accurate fit. The simulated and measured results show that this measurement fixture is able to provide reliable measurements over the UWB frequency band from 3 to 10 GHz. Furthermore, different measurement distances from 230 to 600 μm are found to have similar attenuations at low frequencies, while obvious effects of capacitive coupling are observed over high frequencies. To avoid such effects on measured substrate noise the capacitance between the substrate and the ground of the measurement setup should be minimized. Finally, the presented measurement fixture is validated by measuring the switching noise generated by a practical class-E PA.

Acknowledgements The authors thank the Danish Research Council for Technology and Production Sciences (FTP) for provision of grant support, Daniel Sira for design of the class-E PA, Yonghui Huang for helpful discussion and Peter Boie Jensen for bonding of the chip.

References

1. Granelli, F., & Zhang, H. (2005). Cognitive ultra wide band radio: A research vision and its open challenges. *2nd international workshop on networking with ultra wide band (NEUWB2)* (pp. 55–59). Rome, July 2005.
2. Razavi, B., Aytur, T., Lam, C., Yang, F., Li, K., Yan, R., Kang, H., Hsu, C., & Lee, C. (2005). A UWB CMOS transceiver. *IEEE Journal of Solid-State Circuits, 40*(12), 2555–2562.
3. Gharpurey, R., & Meyer, R. (1996). Modeling and analysis of substrate coupling in integrated circuits. *IEEE Journal of Solid-State Circuits, 31*(3), 344–353.
4. Su, D., Loinaz, M., Masui, S., & Wooley, B. (1993). Experimental results and modeling techniques for substrate noise in mixed-signal integrated circuits. *IEEE Journal of Solid-State Circuits, 28*(4), 420–430.
5. Kristiansson, S., Kagganti, S., Ewert, T., Ingvarson, F., Olsson, J., & Jeppson, K. (2003). Substrate resistance modeling for noise coupling analysis. *International conference on microelectronic test structures* (pp. 124–129). Monterey, CA, March 2003.
6. Pfost, M., & Rein, H. (1998). Modeling and measurement of substrate coupling in Si-bipolar ICs up to 40 GHz. *IEEE Journal of Solid-State Circuits, 33*(4), 582–591.
7. Pfost, M., Rein, H., & Holzwarth, T. (1996). Modeling substrate effects in the design of high-speed Si-bipolar ICs. *IEEE Journal of Solid-State Circuits, 31*(10), 1493–1501.
8. van Heijningen, M., Compiet, J., Wambacq, P., Donnay, S., Engels, M., & Bolsens, I. (2000). Analysis and experimental verification of digital substrate noise generation for epi-type substrates. *IEEE Journal of Solid-State Circuits, 35*(7), 1002–1008.
9. van Heijningen, M., Badaroglu, M., Donnay, S., Gielen, G., & De Man, H. (2002). Substrate noise generation in complex digital systems: Efficient modeling and simulation methodology and experimental verification. *IEEE Journal of Solid-State Circuits, 37*(8), 1065–1072.
10. Makie-Fukuda, K., Kikuchi, T., Matsuura, T., & Hotta, M. (1995). Measurement of digital noise in mixed-signal integrated circuits. *IEEE Journal of Solid-State Circuits, 30*(2), 87–92.
11. Gharpurey, R. (1995). A methodology for measurement and characterization of substratenoise in high frequency circuits. *Proceedings of the IEEE custom integrated circuits* (pp. 487–490). San Diego, CA, May 1999.

Ming Shen received his M.Sc.E.E. degree in 2005 from the Graduate School of Chinese Academy of Sciences, China. He is currently a Ph.D. student at the Department of Electronic Systems, Aalborg University, Denmark, working on substrate noise modelling and suppression in mixed-signal ICs. From 2005 to 2007, he worked as a teaching assistant with the Department of Electronic Engineering, Chinese University of Hong Kong, focusing on wireless location and design of RF modules using LTCC. His current research interests include modelling and suppression of substrate noise and design of RF integrated circuits for wireless systems.

Tian Tong received the B.S.E.E. degree in Microelectronics in 1990, M.S.E.E. degree in Circuit and system in 1995 and Ph.D. degree in Microelectronics in 1998, respectively. He was involved in RF system and its IC implementation since his Ph.D. degree program. Currently he serves as Associate Professor with Aalborg University. The research area focuses on design and implementation of CMOS RF integrated circuit and system, Ultra-wide band transceiver architecture and its CMOS implementation as well as design and implementation of Mixed-signal circuit and system.

Jan H. Mikkelsen received the M.Sc. and Ph.D. degrees in Electrical Engineering from Aalborg University, Denmark in 1995 and 2005, respectively. Since 2001 he has been working as an IC design manager for the large-scale RF-IC design effort at Aalborg University where he currently holds a position as Associate Professor. He has authored or co-authored over 40 peer-reviewed journal and conference papers. His main research interests include analog circuit design, RF/LF CMOS circuit design for various communication applications as well as system level analysis of transceiver architectures. He serves as a reviewer for the IEE and IEEE.

Torben Larsen received the M.Sc. and Dr.Techn. degrees from Aalborg University, Aalborg, Denmark, in 1988 and 1998, respectively. Since 2001, he has been a Full Professor with Aalborg University. He has industrial experience with Bosch Telecom and Siemens Mobile Phones. In 2005, he was appointed member of the Research Council for Technology and Production by the Minister of Science, Technology, and Innovation. He has authored or co-authored over 75 peer-reviewed journal and conference papers. His research interests include RF system design, integrated circuit design, wireless communications, and transceiver design.